3.4

ANALYSIS OF TROPOSPHERIC TEMPERATURE DATA VIA RADIOSONDE WIND DATA IN THE WESTERN TROPICAL PACIFIC

Robert J. Allen* and Steven C. Sherwood
Dept. of Geology and Geophysics, Yale University, New Haven, CT

1. INTRODUCTION

Climate model simulations, when forced with a combination of anthropogenic and natural factors, predict tropospheric warming and stratospheric cooling, with maximum warming in the tropical middle and upper troposphere Tett et al. (2002). This is consistent with radiosonde data since the early 1960's and moist adiabatic lapse rate (MALR) theory. Since the satellite era, however, warming at the surface exceeds that in the troposphere, in particular for the tropics and southern hemisphere (Gaffen et al., 2000; Thorne et al., 2005; Santer et al., 2005). This inconsistency between temperature trends at the surface and troposphere has raised concern about the ability of climate models to predict climate change, the reality of anthropogenic climate change, and especially, the homogeneity of satellite and radiosonde temperature data.

Several authors have documented non-climatic inhomogeneities in the radiosonde temperature archive (Gaffen, 1994; Eskridge et al., 1995; Lanzante et al., 2003a). Current methods used to homogenize the radiosonde data have followed very different identification and adjustment strategies. Such methods often yield significantly different homogenized time series, with the difference between the trends produced by these methods is as large as the trends themselves Free et al. (2002).

In general, the adjustments applied to the radiosonde data have helped alleviate this discrepancy between surface and tropopsheric warming (i.e. adjustments yield more tropospheric warming) (Lanzante et al., 2003b; Thorne et al., 2005). The adjusted data are still inconsistent with models, but it is likely that many undetected problems still remain (Lanzante et al., 2003b; Sherwood et al., 2005).

Analysis of the wind field offers an alternative approach to the monitoring of climate change. For example, Pielke et al. (2001) analyzes trends in the 200 hPa winds (based on NCEP Reanalysis data), looking for changes in the atmospheric circulation. They show that since 1958, the 200 hPa westerly flow has increased at most higher latitudes. According to thermal wind balance, this indicates an increase in the vertically averaged, horizontal gradient of tropospheric temperature. This strategy depends on (1) errors in the wind field being sufficiently small and independent of those in temperature, and (2) climate changes being approximately geostrophically balanced. The former condition is unlikely to hold in reanalyses.

Similar to Pielke et al. (2001), we investigate the thermal wind balance between 850 and 300 hPa. However, we use 70 radiosondes from the Integrated Global Radiosonde Archive (IGRA) Durre et al. (2005). The radiosondes are located in the western tropical Pacific, where the discrepancy between surface and tropospheric temperature trends is large.

2. METHODOLOGY

Analysis of the wind field offers an alternative approach to the monitoring of atmospheric temperature and its change over time. Assuming geostrophic and hydrostatic balance, the thermal wind equation (TWE) relates the vertical wind shear to the horizontal gradient of temperature. Integration of the east-west component of the TWE, for a layer bounded by two isobaric surfaces, yields a relationship between the meridional gradient of the height difference between the top and bottom of the layer, and the corresponding difference between the westerly geostrophic wind ($\triangle$u):

$$\frac{d\triangle z}{dy} = -\frac{f}{g}\triangle u. \quad (1)$$

Here, $\triangle$z is the height difference between the top and bottom of the layer (also referred to as the thickness of the layer), f is the Coriolis parameter and g is the acceleration of gravity. An equivalent equation to (1) holds for the perpendicular, north-south direction. To get the meridional gradient of $\triangle$z based on the wind field from (1), each station's annual monthly mean zonal (u) wind component is interpolated onto a regularly spaced grid using anisotropic ordinary kriging Isaaks and Srivastava (1989). Parameters of the kriging proceduresuch as the ranges and nuggetare optimized using a jackknife procedure. For example, the (station and annual average) RMS error of $\triangle$u is minimized (equal to 2.9 m/s) for a longitudinal range of 9250 km and a latitudinal range of 3250 km. At each grid point, $\triangle$u is calculated, and (1) is used to estimate the meridional gradient of $\triangle$z. Similarly, the observed $\triangle$z is calculated at each grid point by kriging the observed thickness at each station. As with the kriging of $\triangle$u, a jackknife procedure is used to estimate optimum thickness kriging parameters. Finite differences are then used to estimate the meridional gradient of $\triangle$z. Thickness $\triangle$z and layer mean temperature ($\bar{T}$) are related via the hypsometric equation

$$\triangle z = \frac{R_d}{g}\ln(\frac{p_0}{p_1})\bar{T}. \quad (2)$$

Here, R_d is the gas constant for dry air and $p_0 > p_1$. Substituting (2) into (1) yields

$$\frac{d\bar{T}}{dy} = -\frac{f}{g}\ln(\frac{p_1}{p_0})\triangle u. \quad (3)$$

Equation (3) states that as the north-south temperature gradient decreases (increases), the vertical westerly shear of the geostrophic wind also decreases (increases). A decrease in upper level (or increase in lower level) wind speeds would be expected anywhere the usual equator-to-pole temperature gradient became weaker.

3. RESULTS

The accuracy of (1), in terms of the long-term mean, is tested in Fig. 1a. The wind-estimated meridional thickness gradient ($\triangle z^u_\phi$) is very similar to the corresponding thickness gradient derived from the observed heights ($\triangle z^T_\phi$). Values from 0 m/degree-latitude near the equator to 18 m/degree-latitude over the Australian continent, consistent with maximum baroclinicity in mid-latitude regions. The largest disagreement between $\triangle z^u_\phi$ and $\triangle z^T_\phi$ occurs on the southern periphery of the domain, where $\triangle z^T_\phi < \triangle z^u_\phi$. This may be due to a lack of data, especially for the southwest corner of the study area. Based on station locations, the median absolute percent error ($\triangle z^T_\phi$-$\triangle z^u_\phi$) is 15% and the median percent error is 2%.

Fig. 1b illustrates the ability of the TWE to capture the long-term mean seasonal (summer minus winter) baroclinic variability.

*Corresponding author address: Robert J. Allen, P.O. Box 208109, Yale University, New Haven, CT, 06520; e-mail: robert.allen@yale.edu

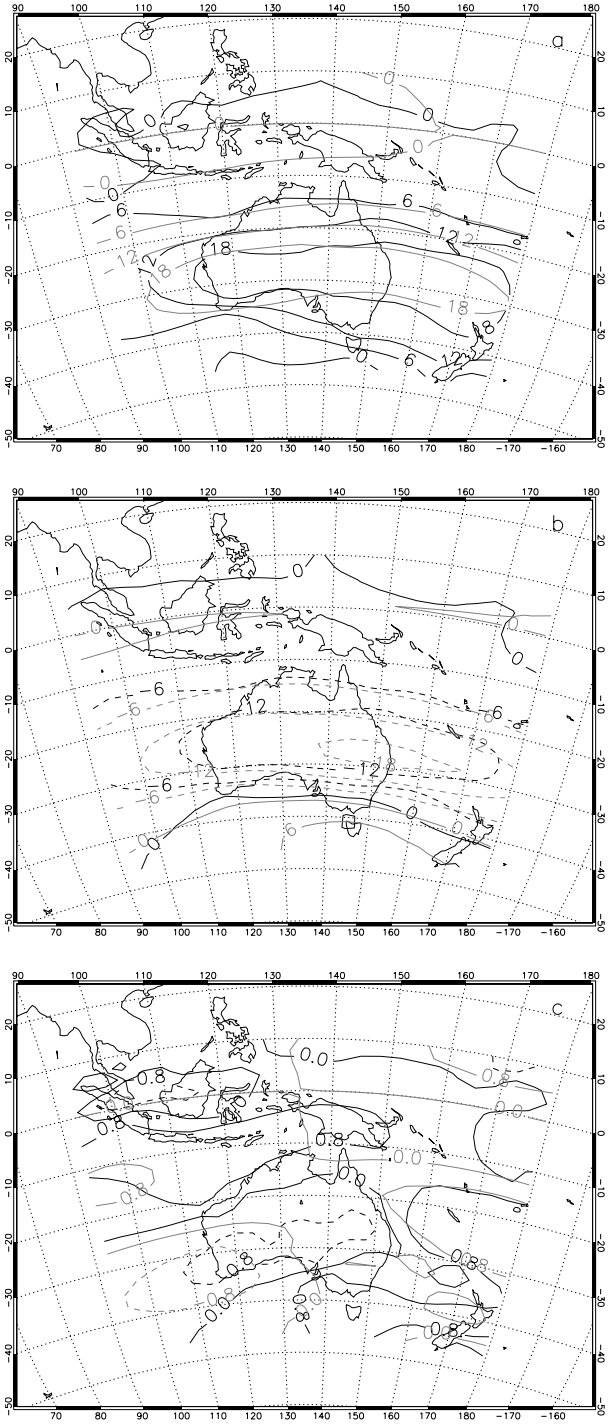

FIG. 1: . Observed (black) and wind-estimated (gray) meridional thickness gradients for the a. long term (annual) mean; b. long term seasonal (summer minus winter) difference; and c. ESNO (warm minus cold) signal. All plots are based on the 300 and 850 hPa pressure surfaces at 0000 UTC. Negative contours are dashed.

Again, there is good correspondence between $\triangle z_\phi^T$ and $\triangle z_\phi^u$. Both show a predominance of negative contours, consistent with greater baroclinicity during winter, and both possess minima less than -12 m/degree-latitude over the Australian continent. Based on station locations, the median absolute percent error is 22% and the median percent error is -3%.

A similar test for variability associated with El Nino-Southern Oscillation (ENSO) is shown in Fig. 1c. Warm (cold) years are defined as those with an annual average Southern Oscillation Index (SOI) less than (greater than) -0.52 (0.83), resulting in 15 warm (5 cold) between 1979 and 2004. In this case, there is less agreement between $\triangle z_\phi^T$ and $\triangle z_\phi^u$. Differences ($\triangle z_\phi^T$ - $\triangle z_\phi^u$) are nearly as large as the signal itself, with an error of at least -0.5 m/degree-latitude over most of the Australian continent (not shown). Unlike the long term mean and seasonal signal, however, the magnitude of the ENSO signal is relatively small.

Fig. 2 shows the trend of zonal means of the two baroclinicity estimates over the satellite era. Based on the zonal winds, the decadal trend of $\triangle z_\phi^u$ assumes values near zero for all latitudes, ranging from about 0.3 m/degree-latitude-decade at 30°S to -0.15 m/degree-latitude-decade at 18°S. The corresponding trend of $\triangle z_\phi^T$, however, exhibits much greater variability. Values range from a maximum of 0.7 m/degree-latitude-decade at 32°S to a minimum of -1.2 m/degree-latitude-decade at 7°S. Throughout most of the tropics and sub-tropics, the trend of $\triangle z_\phi^T$ is negative, ranging from -0.5 to -1 m/degree-latitude-decade.

Integration of the trend of $\triangle z_\phi$ over latitude (beginning at the southernmost point) using (2), gives equivalent trend estimates of $\bar{T}$ from the two methods relative to that at 47°S (upper curves in Fig. 2). The wind-based trend in $\bar{T}$ for most latitudes is near zero (and positive), with a maximum of 0.1°C/decade at 20°S. The trend from reported temperatures is similar throughout the mid-latitudes, with slightly larger minima and maxima. In the tropics and subtropics, however, the two curves diverge substantially, with the observed $\bar{T}$ decreasing to -0.2 to -0.4°C/decade. Hence, relative to mid-latitudes, the trend in observed reaches -0.6°C/decade, whereas the corresponding wind-based trend is at most -0.1°C/decade. These results suggest that the radiosonde temperature data (which the height data is derived from) possesses an artificial cooling bias in the tropical and subtropical troposphere of the western Pacific.

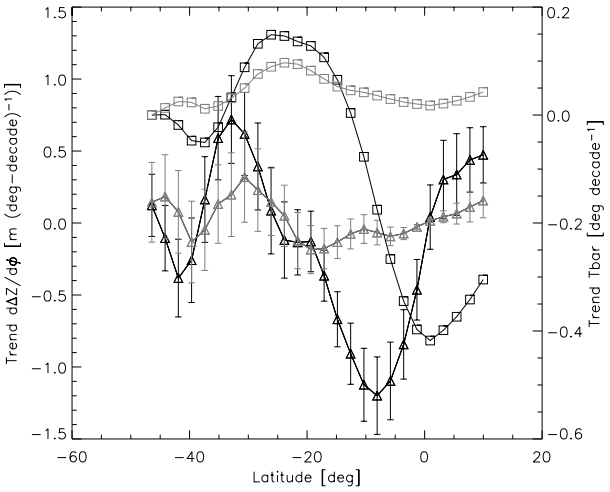

FIG. 2: Latitude versus the linear least-squares trend of the zonal-annual mean meridional thickness gradient (triangles) based on temperature (black) and wind-estimates (gray). Error bars indicate the 1-σ uncertainty in the estimated slope. Also shown is the corresponding decadal trend in vertically-averaged tropospheric temperature (squares). Trends are based on data from 1979-2004.

4. CONCLUSIONS

For tropical and subtropical latitudes in the western Pacific, the observed meridional thickness gradient exhibits a negative trend over the satellite era (1979-2004), while the corresponding meridional thickness gradient based on the winds shows negligible change. This result implies that the corresponding depth averaged (tropospheric) temperature in the tropics and subtropics has decreased relative to that at higher latitudes. This supports the possibility that an artificial cooling bias exists in the tropical radiosonde temperature data. The error implied here is several times larger than the expected tropical trend.

REFERENCES

Durre, I., R. S. Vose, and D. M. Wuertz, 2005: Overview of the integrated global radiosonde archive. *J. Climate*. Submitted.

Eskridge, R. E., O. A. Alduchov, I. V. Chernykh, Z. Panmao, A. C. Polansky, and S. R. Doty, 1995: A comprehensive aerological reference data set (CARDS): Rough and systematic errors. *Bull. Amer. Meteorol. Soc.*, **76**, 1759–1775.

Free, M., I. Durre, E. Aguilar, D. Seidel, T. C. Peterson, R. E. Eskridge, J. K. Luers, D. Parker, M. Gordon, J. R. Lanzante, S. A. Klein, J. R. Christy, S. Schroeder, B. J. Soden, L. M. McMillin, , and E. Weatherhead, 2002: Creating climate reference datasets: CARDS workshop on adjusting radiosonde temperature data for climate monitoring. *Bull. Amer. Meteor. Soc.*, **83**, 891–899.

Gaffen, D. J., 1994: Temporal inhomogeneities in radiosonde temperature records. *J. Geophys. Res.*, **99**, 3667–3676.

Gaffen, D. J., B. D. Santer, J. S. Boyle, J. R. Christy, N. E. Graham, and R. J. Ross, 2000: Multidecadal changes in the vertical temperature structure of the tropical troposphere. *Science*, **287**, 1242–1245.

Isaaks, E. H. and R. M. Srivastava, 1989: *An Introduction to Applied Geostatistics*. Oxford University Press, 561 pp.

Lanzante, J. R., S. A. Klein, and D. J. Seidel, 2003a: Temporal homogenization of monthly radiosonde temperature data. Part I: Methodology. *J. Climate*, **16**, 224–240.

Lanzante, J. R., S. A. Klein, and D. J. Seidel, 2003b: Temporal homogenization of monthly radiosonde temperature data. Part II: Trends, sensitivities, and MSU comparison. *J. Climate*, **16**, 241–262.

Pielke, R. A., T. N. Chase, T. G. F. Kittel, J. A. Knaff, and J. Eastman, 2001: Analysis of 200 mbar zonal winds for the period 1958-1997. *J. Geophys. Res.*, **106**, 27,287–27,290.

Santer, B. D., T. M. L. Wigley, C. Mears, F. J. Wentz, S. A. Klein, D. J. Seidel, K. E. Taylor, P. W. Thorne, M. F. Wehner, P. J. Gleckler, J. S. Boyle, W. D. Collins, K. W. Dixon, C. Doutriaux, M. Free, Q. Fu, J. E. Hansen, G. S. Jones, R. Ruedy, T. R. Karl, J. R. Lanzante, G. A. Meehl, V. Ramaswamy, G. Russell, and G. A. Schmidt, 2005: Amplification of surface temperature trends and variability in the tropical atmosphere. *Science*, **309**, 1551–1556.

Sherwood, S. C., J. R. Lanzante, and C. L. Meyer, 2005: Radiosonde daytime biases and late-20th century warming. *Science*, **309**, 1556–1559.

Tett, S. F. B., G. S. Jones, P. A. Stott, D. C. Hill, J. F. B. Mitchell, M. R. Allen, W. J. Ingram, T. C. Johns, C. E. Johnson, A. Jones, D. L. Roberts, D. M. H. Sexton, and M. J. Woodage, 2002: Estimation of natural and anthropogenic contributions to twentieth century temperature change. *J. Geophys. Res.*, **107**, 10.1029/2000JD000028.

Thorne, P. W., D. E. Parker, S. F. B. Tett, P. D. Jones, M. McCarthy, H. Coleman, and P. Brohan, 2005: Revisiting radiosonde upper-air temperatures from 1958-2002. *J. Geophys. Res.*, **110**, 10.1029/2004JD005753.